Diabetologia (2013) 56:2222–2230
DOI 10.1007/s00125-013-2978-x

ARTICLE

SDF-1–CXCR4 differentially regulates autoimmune diabetogenic T cell adhesion through ROBO1–SLIT2 interactions in mice

John D. Glawe · Eleni M. Mijalis · William C. Davis · Shayne C. Barlow · Neslihan Gungor · Robert McVie · Christopher G. Kevil

Received: 15 March 2013 / Accepted: 7 June 2013 / Published online: 28 June 2013

Abstract
Aims/hypothesis We had previously reported that stromal cell-derived factor 1 (SDF-1) mediates chemorepulsion of diabetogenic T cell adhesion to islet microvascular endothelium through unknown mechanisms in NOD mice. Here we report that SDF-1-mediated chemorepulsion occurs through slit homologue (SLIT)2-roundabout, axon guidance receptor, homologue 1 (*Drosophila*) (ROBO1) interactions.
Methods C-X-C receptor (CXCR)4 and ROBO1 protein expression was measured in mouse and human T cells. Parallel plate flow chamber adhesion and detachment studies were performed to examine the molecular importance of ROBO1 and SLIT2 for SDF-1-mediated T cell chemorepulsion. Diabetogenic splenocyte transfer was performed in NOD/LtSz *Rag1*$^{-/-}$ mice to examine the effect of the SDF-1 mimetic CTCE-0214 on adoptive transfer of diabetes.
Results CXCR4 and ROBO1 protein expression was elevated in diabetic NOD/ShiLtJ T cells over time and coincided with the onset of hyperglycaemia. CXCR4 and ROBO1 expression was also increased in human type 1 diabetic T cells, with ROBO1 expression maximal at less than 1 year post diagnosis. Cell detachment studies revealed that immunoneutralisation of ROBO1 prevented SDF-1-mediated chemorepulsion of NOD T cell firm adhesion to TNFα-stimulated islet endothelial cells. SDF-1 increased NOD T cell adhesion to recombinant adhesion molecules, a phenomenon that was reversed by recombinant SLIT2. Finally, we found that an SDF-1 peptide mimetic prevented NOD T cell adhesion in vitro and significantly delayed adoptive transfer of autoimmune diabetes in vivo.
Conclusions/interpretation These data reveal a novel molecular pathway, which regulates diabetogenic T cell recruitment and may be useful in modulating autoimmune diabetes.

Keywords Adhesion molecules · Cell adhesion · Chemorepulsion · Leucocyte recruitment

Abbreviations

CXCR	C-X-C receptor
HBSS	Hanks' balanced salt solution
ICAM-1	Intercellular cell adhesion molecule 1
ROBO	Roundabout, axon guidance receptor
SDF-1	Stromal cell-derived factor 1
SLIT	Slit homologue
TBS	TRIS buffered saline
VCAM-1	Vascular cell adhesion molecule 1

Introduction

Stromal cell-derived factor 1 (SDF-1), also known as C-X-C ligand 12, is a small, 8 kDa chemokine involved in leucocyte activation and chemotaxis. The receptors for SDF-1 are C-X-C receptor (CXCR)7 [1] and CXCR4, the latter of which only binds SDF-1 and ubiquitin [2]. CXCR7 possesses a tenfold higher affinity for SDF-1 than CXCR4 [1]; however, it is expressed at very low levels on T cells [3]. In vivo SDF-1 promotes cell adhesion, transendothelial migration and chemotaxis. However, we and others have previously reported

Electronic supplementary material The online version of this article (doi:10.1007/s00125-013-2978-x) contains peer-reviewed but unedited supplementary material, which is available to authorised users.

J. D. Glawe · E. M. Mijalis · W. C. Davis · C. G. Kevil (✉)
Department of Pathology, LSU Health-Shreveport,
1501 Kings Highway, Shreveport, LA 71130, USA
e-mail: ckevil@lsuhsc.edu

S. C. Barlow
Department of Animal Resources, University of South Carolina School of Medicine, Columbia, SC, USA

N. Gungor · R. McVie
Department of Pediatrics, Pediatric Endocrinology,
LSU Health-Shreveport, Shreveport, LA, USA

that SDF-1 can mediate chemorepulsion responses that may be of pathophysiological importance [4–6].

Several agonists and antagonists that interact with CXCR4 have been developed. The small peptide agonist CTCE-0214 increases migration of $CD34^+$ cells, although at much higher concentrations than SDF-1 [7], and is beneficial in systemic inflammation [8], while the peptide antagonist CTCE-9908 increases uropod formation, but has no effect on migration or adhesion [9]. Disruption of SDF-1–CXCR4 binding by the CXCR4 antagonist AMD3100 accelerates the development of diabetes in adoptive transfer models [10] and induces beta cell apoptosis [11].

SDF-1 is involved in recruitment of T cells to the pancreas in type 1 diabetes [12]. The injection of mice with antibodies against SDF-1 alters the development of diabetes and suppression of insulitis [13]. We previously demonstrated that SDF-1 produced different effects on NOD and C57BL/6J mouse T cell adhesion under shear stress in vitro, promoting adhesion and reducing detachment of C57BL/6J T cells, while decreasing adhesion and increasing detachment of NOD T cells [4]. However, the mechanisms regulating this response remain unknown.

Members of the SLIT protein family are large glycoproteins that are important for nervous system development, but can be expressed by epithelial [14] and endothelial cells [15]. The SLIT molecules (SLIT1, SLIT2 and SLIT3) bind with members of the roundabout, axon guidance receptor (ROBO) family of receptors and interact with heparan sulphate chains [16]. In retinal axons in vivo, SDF-1 has been shown to modulate SLIT and ROBO signalling [17], while in leucocytes SLIT2 may modulate SDF-1-mediated chemotaxis [14, 18, 19], transendothelial migration and adhesion of T cells [13], and migration of dendritic cells [15].

In this study we examined the mechanisms of SDF-1-induced detachment of NOD T cells and the role of SLIT–ROBO interactions in this response. We also evaluated whether an SDF-1 peptide mimetic could affect the development of adoptive transfer of diabetes in NOD/LtSz *Rag1*$^{-/-}$ mice. Finally, we investigated whether alterations in CXCR4 and ROBO1 were unique to mouse T cells or also occurred in human T cells.

Methods

Animals Mice were housed at the Louisiana State University Health Sciences Center (LSUHSC)-Shreveport Animal Resource Facility, which is accredited by the Association for Assessment and Accreditation of Laboratory Animal Care, and maintained according to the National Research Council Guide for Care and Use of Laboratory Animals. Experiments were conducted in compliance with the Institutional Animal Care and Use Committee. Female NOD/ShiLtJ, NOD/LtSz *Rag1*$^{-/-}$ and C57BL/6J mice were purchased from the Jackson Laboratory (Bar Harbor, ME, USA). Cohorts of NOD/ShiLtJ mice were killed at 6, 12, 18 and 22 weeks to examine protein and gene expression changes during the progression of autoimmune diabetes.

T cell isolation CD3 T cells isolated from splenocytes of female NOD/ShiLtJ or C57BL/6J mice were negatively selected using a kit (EasySep Mouse T Cell Enrichment; Stem Cell Technologies, Vancouver, BC, Canada). For human T cells, blood was drawn from either type 1 (n=16) or type 2 diabetic (n=5) patients, or from healthy controls (n=11) after participants had given informed consent and procedures had been approved by the Institutional Review Board at LSUHSC-Shreveport (Protocol H08-070). T cells were negatively selected from 20 ml blood using a RosetteSep human T cell enrichment cocktail (Stem Cell Technologies).

Western blots T cells were isolated as described above and lysed in radioimmunoprecipitation assay buffer (50 mmol/l TRIS-HCl, pH 8.0, 150 mmol/l NaCl, 1% vol./vol. Nonidet-40, 0.5% wt/vol. deoxycholate and 0.1% wt/vol. SDS) supplemented with 0.1 μmol/l leupeptin, 0.3 μmol/l aprotinin and 1 μmol/l phenylmethylsulfonyl fluoride. Whole-cell protein homogenates (12.5 μg total protein) were loaded on 10% polyacrylamide SDS gels and electrophoresis was performed. Gels were transferred overnight to Immobilon-P7 (Bio-Rad, Hercules, CA, USA) and subsequent membranes were blocked for 2 h with 5% wt/vol. BSA (ROBO1) or 5% wt/vol. non-fat dry milk (CXCR4) in TRIS buffered saline (TBS). Membranes were incubated overnight at 4°C with antibodies against ROBO1 (vRobo1; Developmental Studies Hybridoma Bank, Iowa City, IA, USA) or CXCR4 (ab2074; Abcam, Cambridge, MA, USA) at a dilution of 1:100 (0.27 μg/ml) or 1:500, respectively, in blocking buffer supplemented with 0.1% vol./vol. Tween-20. The remaining washes and incubations were performed at room temperature in TBS containing 0.1% wt/vol. milk and 0.1% vol./vol. Tween-20. To validate the specificity of the CXCR4 antibody, additional blots were also preincubated with and without an equal concentration of the CXCR4 peptide (ab8126; Abcam), which served as the immunogen for the antibody.

For ROBO1, membranes were washed three times for 5 min and incubated for 2 h at room temperature with peroxidase-conjugated anti-mouse IgM secondary antibody (A8786; Sigma-Aldrich, St Louis, MO, USA) at a dilution of either 1:2,000 (mouse) or 1:500 (human). For CXCR4, membranes were washed as above and incubated for 2 h with peroxidase-conjugated anti-rabbit antibody (A0545; Sigma-Aldrich) at 1:2,000 dilution. After three 10 min washes, membranes were rinsed for 10 min in TBS. Chemiluminescence was performed using enhanced chemiluminescence detection reagents (GE Healthcare, Little Chalfont, UK). Various exposures to Hyblot film (E3018; Denville Scientific, South Plainfield, NJ, USA)

were performed to ensure exposure linearity. Films were scanned and quantified using Image J (National Institutes of Health, Bethesda, MD, USA), with densitometric values being normalised to actin expression and reported as means ± SEM.

Flow cytometry Splenocytes were isolated as above, Fc-blocked for 15 min at room temperature with 5 μg/10^6 cells of anti-mouse CD16/CD32 (14-0161-82; eBioscience, San Diego, CA, USA) and incubated for 20 min at room temperature with 0.8 μg/10^6 cells of allophycocyanin-conjugated anti-mouse CXCR7 clone 11G8 (FAB4227A; R&D Systems, Minneapolis, MN, USA) and 0.3 μg/10^6 cells of FITC-conjugated anti-mouse CD3 (553062; BD Biosciences, San Jose, CA, USA). Cells were rinsed twice in PBS containing 2% vol./vol. FBS, and 10,000 events per sample were collected and analysed using FacsCalibur (BD Biosciences) and CellQuest software (BD Biosciences).

RNA isolation and quantitative RT-PCR Quantitative RT-PCR analysis was performed as previously reported by our laboratory [20]. Total RNA was isolated using a kit (RNeasy Isolation Kit; Qiagen, Hilden, Germany). Reverse transcription was carried out using 1 μg total RNA from each sample. Primers for *Cxcr4* and *Robo1* were designed with a software package (Beacon Designer, Premier Biosoft, Palo Alto, CA, USA) with sequences as listed in electronic supplementary material (ESM) Table 1. A 40-fold dilution of cDNA was used as a template to perform quantitative RT-PCR with iQ SYBR Green Supermix (Bio-Rad). *Gapdh* was used as the internal control gene for the reactions. The threshold cycle (C_t) formula was used to calculate changes in gene expression.

Cell culture MS1 mouse pancreatic islet endothelial cells (CRL-2279; ATCC, Manassas, VA, USA) were cultured in DMEM supplemented with L-glutamine, penicillin, streptomycin and 5% vol./vol. FBS (Atlanta Biologicals, Lawrenceville, GA, USA). Culturing was done in 5% CO_2 at 37°C. Cells were grown to confluence in T75 flasks and seeded in 35 mm tissue culture dishes.

In vitro hydrodynamic flow chamber adhesion assays Hydrodynamic flow chamber assays were performed as previously described [4]. Briefly, T cells isolated as described above were labelled with CellTracker Green (C7025; Life Technologies, Carlsbad, CA, USA), rinsed and resuspended at a concentration of 2×10^5 cells/ml in phenol red-free Hanks' balanced salt solution (HBSS). The cells were placed in a beaker previously coated with Sigmacote (Sigma-Aldrich), kept at 37°C and stirred at 60 rev/min. A flow chamber insert and gasket with a 0.5 cm flow width and 250 μm thickness (GlycoTech, Gaithersburg, MD, USA) were used with 35 mm cell culture dishes containing confluent MS1 cell cultures to form a parallel plate flow chamber. To activate the endothelium, MS1 cells were treated for 4 to 6 h at 37°C with 10 ng/ml recombinant mouse TNFα (T7539; Sigma).

For the SDF-1 peptide mimetic T cell adhesion assay, MS1 cells were rinsed with HBSS and treated for 10 min with an SDF-1 peptide mimetic [21] (sequence AYWKENKEQ with two branched lysines) at 0.5, 1, 5 or 10 μg/ml. T cells were pulled through polypropylene tubing by a syringe pump (KD Scientific, Holliston, MA, USA) across the endothelial monolayer at a physiological shear stress of 150 mPa. Real-time digital video images (minimum 28 frames/s) were captured with an epifluorescence microscope (TE-2000 Eclipse; Nikon, Tokyo, Japan) and digital camera (Model C4742-95-12ER: Hamamatsu Photonics, Hamamatsu, Japan). Simple PCI software (Hamamatsu Photonics) was used to analyse the video and extract T cell rolling velocities. Cells were considered firmly adherent if they remained stationary for 10 s within the field of view. A minimum of three videos per plate and four plates per condition were used for analysis.

T cell detachment assays were performed as previously reported by us [4]. Briefly, T cells were injected into the tubing via an inlet port upstream of the flow chamber at a concentration of 2×10^6 cells/ml and allowed to firmly adhere under static conditions for 15 min. Next, the shear stress was initiated and increased in a step-wise manner every 30 s as follows: 35, 56, 91, 224, 504 and 980 mPa. The assay was recorded by video, which was analysed to determine the percentage of cells detached at the end of each shear stress interval. For the anti-ROBO1 detachment assay, MS1 cells were treated for 10 min at 37°C with TNFα as described above and then with 100 ng/ml recombinant mouse SDF-1α (460-SD; R&D Systems). T cells were pretreated for 30 min at 37°C with 20 μg/ml ROBO1 blocking antibody (GT15144; Neuromics, Edina, MN, USA) or isotype control (GT15900; Neuromics).

In the SLIT2 detachment assay, the following modifications were made. Vascular cell adhesion molecule 1 (VCAM-1)- and intercellular cell adhesion molecule 1 (ICAM-1)-coated plates were substituted for confluent monolayers of MS1 cells to isolate the specific ligand and receptor interactions involved. Plates were treated by tracing five 5 mm diameter circles aligned in one row in the centre of a 100 mm diameter tissue culture dish using a PAP pen, and then applying 15 μl of 1 mg/ml protein A to each circle for 30 min. Plates were rinsed twice with PBS and blocked for 30 min with 5% wt/vol. BSA in PBS. Plates were rinsed and each circle then treated for 30 min with 15 μl of a solution containing 5 μg/ml ICAM-1/Fc chimera (796-IC; R&D Systems) and 5 μg/ml VCAM-1/Fc chimera (643-VM; R&D Systems), or PBS (control). Plates were rinsed and stored at 4°C. T cells were suspended in HBSS containing 10 μg/ml heparin sodium and treated for 15 min at 37°C with 250 ng/ml SDF-1 and 20 μg/ml recombinant mouse SLIT2 (5444-SL; R&D Systems) before use. A Glycotech rectangular flow chamber with 250 μm thick gasket and 1 cm wide flow path was used.

Diabetes adoptive transfer Single cell suspensions of splenocytes were isolated from spleens of spontaneously diabetic female NOD/ShiLtJ mice as described previously [22]. Erythrocytes were lysed with 150 mmol/l NH_4Cl, 1.0 mmol/l $KHCO_3$ and 0.1 mmol/l disodium EDTA, and resuspended in PBS at 200×10^6 splenocytes per ml. Female NOD/LtSz *Rag1*$^{-/-}$ mice were injected retro-orbitally with 20×10^6 splenocytes. Recipient mice were injected retro-orbitally, either once or three times per week, with the SDF-1 peptide mimetic CTCE-0214 (sequence KPVSLSYRCPCRFF-Linker-LKWIQEYLEKALN-OH) (British Canadian BioSciences, Vancouver, BC, Canada) at 1 or 10 mg/kg, or with PBS. Blood glucose was measured twice per week (Ascensia Glucometer Elite; Bayer, Leverkusen, Germany) from a tail stick. Mice were considered hyperglycaemic following two consecutive measurements at 13.9 mmol/l (250 mg/dl) glucose.

Results

CXCR4, ROBO1 and CXCR7 expression We first investigated whether different expression levels of CXCR4, the receptor for SDF-1, occur in T cells from C57BL/6J and diabetes-prone NOD/ShiLtJ mice at 12 weeks of age. NOD/ShiLtJ mice showed an increase in expression of CXCR4 in T cells vs C57BL/6J mice (Fig. 1a). We then examined T cell expression levels of ROBO1, a receptor for SLIT2 that is known to modulate the signalling effects of SDF-1 and CXCR4. NOD/ShiLtJ mice showed a significant increase in ROBO1 T cell expression levels over that of C57BL/6J mice (Fig. 1b). These data indicate that the contrasting effects of SDF-1 on C57BL/6J and NOD/ShiLtJ mice are possibly the result of the different levels of CXCR4 and ROBO1 expressed on their T cells. To determine whether SDF-1 was likely to have an effect by signalling through CXCR7, we dual-stained splenocytes from NOD/ShiLtJ and C57BL/6J mice with anti-mouse CD3 and anti-mouse CXCR7, and analysed them by flow cytometry. Staining for CXCR7 in CD3$^+$ cells was minimal in both strains of mice (Fig. 1c, d).

Having determined that NOD/ShiLtJ CD3 T cells have increased CXCR4 and ROBO1, we investigated whether protein and mRNA levels changed during the time course of disease progression. As shown in Fig. 2a, NOD/ShiLtJ mice become hyperglycaemic by 18 weeks of age. Western blots of T cell lysates for CXCR4 and ROBO1 (Fig. 2b) were quantified by densitometric analysis. Protein levels of CXCR4 and ROBO1 progressively increased between 12 and 22 weeks of age (Fig. 2c, d). However, mRNA expression of *Cxcr4* significantly decreased over time during diabetes progression (Fig. 2e), while mRNA expression of *Robo1* remained unchanged (Fig. 2f).

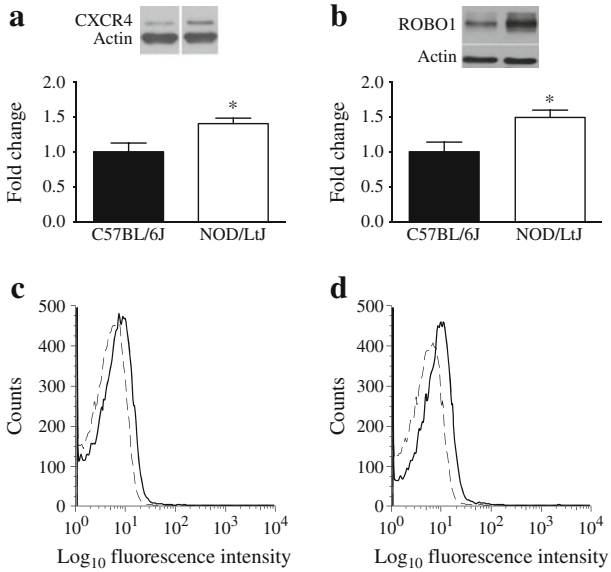

Fig. 1 (**a**) Densitometric analysis, with representative western blots, showing increased expression of CXCR4 and (**b**) ROBO1 in T cells from 12-week-old NOD/ShiLtJ (LtJ) mice over that from T cells of C57BL/6 J mice (*$p<0.05$). (**c**) Flow cytometric analysis of T cells from C57BL/67 and (**d**) NOD/ShiLtJ mice showed only low-level staining for extracellular CXCR7 (solid line) with isotype controls (dashed line)

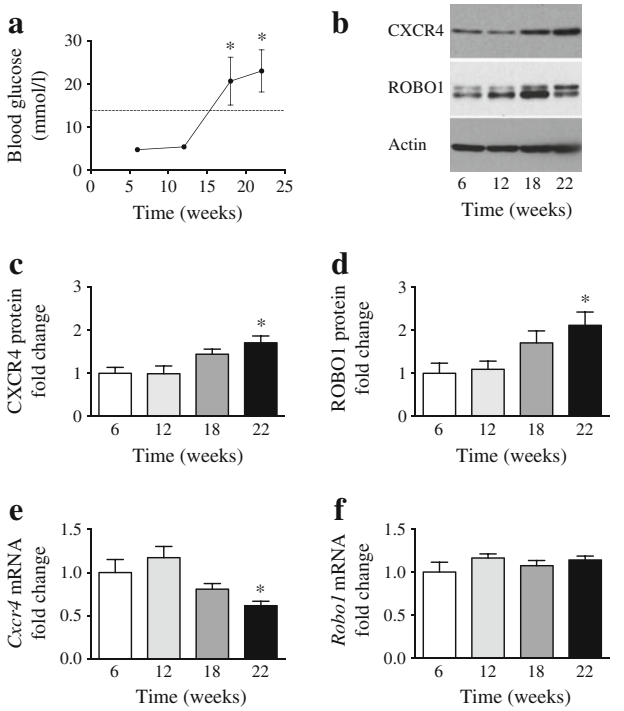

Fig. 2 (**a**) NOD/ShiLtJ mice develop significantly increased blood glucose levels by 18 weeks of age. The dashed line at 13.9 mmol/l glucose (250 mg/dl) denotes the threshold for hyperglycaemia. (**b**) Western blots for CXCR4 and ROBO1 in NOD/ShiLtJ T cells showing significantly increased (**c**) CXCR4 and (**d**) ROBO1 protein at 22 weeks of age vs 6 and 12 weeks of age as measured by densitometric analysis. (**e**) mRNA expression in T cells of *Cxcr4* was significantly decreased at 22 weeks of age compared with 12 weeks of age, whereas (**f**) mRNA expression of *Robo1* in T cells was unchanged. (**a**, **c**–**e**) *$p<0.05$

Human type 1 diabetic patients have increased T cell CXCR4 and ROBO1 expression Next, we investigated whether a similar increase in CXCR4 and ROBO1 was found in human type 1 diabetic patients. CD3 T cells were purified from blood drawn from human type 1 diabetic patients and non-diabetic controls to measure CXCR4 and ROBO1 expression by western blot of protein lysates. CXCR4 abundance in T cells from type 1 diabetic patients was approximately three times that of non-diabetic controls (Fig. 3a). There was no statistical difference between recently diagnosed type 1 diabetic patients (≤1 year) and those diagnosed at least 1 year previously. A similar increase was also seen for ROBO1 expression in T cells from type 1 diabetic patients compared with those from healthy controls (Fig. 3b). Interestingly, a significant increase in ROBO1 expression occurred in type 1 diabetic participants less than 1 year after diagnosis, subsequently diminishing over time. Figure 3c, d shows that CXCR4 and ROBO1 levels were not elevated in patients recently diagnosed (≤1 year) with type 2 diabetes compared with non-diabetic controls. Table 1 reports patient sex distribution, age, duration of disease, per cent HbA_{1c} and autoantibody positivity.

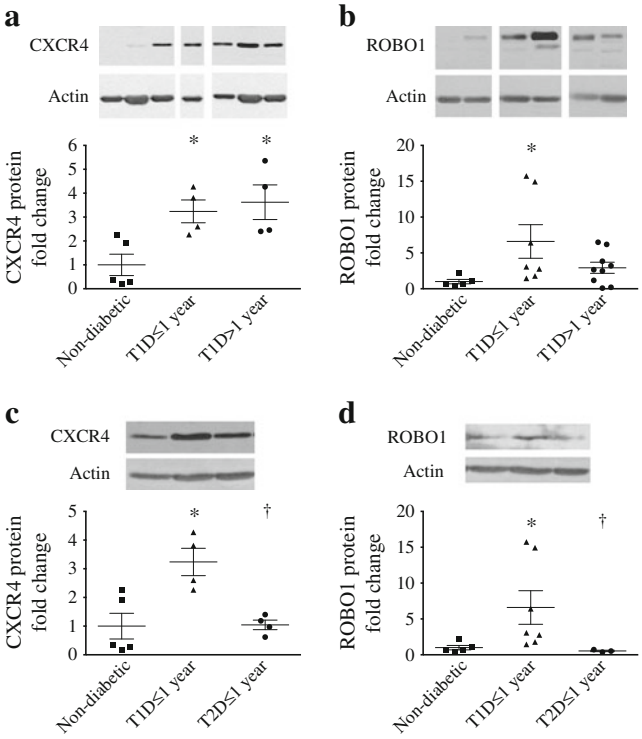

Fig. 3 (**a**) Densitometric analysis of representative western blots showing increased expression of CXCR4 in type 1 diabetic patients with ≤1 year and >1 year disease duration compared with non-diabetic controls; $n=4$ for each diabetes group, $n=5$ for control group; $^{*}p<0.05$. (**b**) Analyses and western blots as above (**a**) showing increased expression of ROBO1 in recently diagnosed type 1 diabetic patients ($n=7$) compared with non-diabetic controls; $n=5$; $^{*}p<0.05$. No statistical significance was seen between either of the above groups and type 1 diabetic patients at more than 1 year after diagnosis ($n=9$). (**c**) Analyses and western blots as above (**a**, **b**) showing no increase in CXCR4 in recently diagnosed type 2 diabetic patients ($n=4$) and a significant difference in CXCR4 levels between recently diagnosed type 1 diabetic patients ($n=4$), and both non-diabetic ($n=5$; $^{*}p<0.05$) and recently diagnosed type 2 diabetic patients ($^{\dagger}p<0.05$). (**d**) No increase in ROBO1 was seen in recently diagnosed type 2 diabetic patients ($n=3$), but significant differences in ROBO1 levels were found between recently diagnosed type 1 diabetic patients ($n=7$) and both non-diabetic ($n=5$; $^{*}p<0.05$) and recently diagnosed type 2 diabetic patients ($\dagger p<0.05$)

Anti-ROBO1 reverses SDF-1-induced detachment of NOD T cells in vitro Having established that T cell levels of ROBO1 differ between C57BL/6J and NOD/ShiLtJ mice, we investigated whether SDF-1-mediated firm adhesion defects were dependent on ROBO1–SLIT2 binding. Using a parallel plate flow chamber detachment assay where NOD/ShiLtJ T cells were allowed to statically adhere to islet endothelial cell monolayers, adherent T cells were subsequently exposed to incrementally increased shear stress to test whether blocking of ROBO1–SLIT2 binding with an anti-ROBO1 antibody would alter T cell adhesion. Figure 4a demonstrates that TNFα stimulation decreased detachment, as expected, compared with unstimulated control, while the addition of treatment with SDF-1 (TNFα+SDF) reduced this adhesive effect. Anti-ROBO1 pretreatment (TNFα+SDF+anti-ROBO1) produced an adhesive effect, indicating that ROBO1 is involved in mediating detachment responses of NOD T cells from SDF-1-treated endothelial cells. The detachment of T cells treated with an isotype control (TNFα+SDF+isotype control) was not significantly different from that of untreated T cells from TNFα+SDF-1-treated endothelial monolayers.

Table 1 Data for diabetic patients

Variable	Type 1	Type 2
Participants (*n*)	15	5
Sex (*n*)		
Male	8	1
Female	7	4
Mean age (years)	10.9 (4–17)	15.7 (14–18)
Diabetes duration (years)	1.8 (0–9)	3.5 (1–5)
HbA_{1c} (%)	10.9 (6.7–16.0)	6.3 (5.1–7.4)
HbA_{1c} (mmol/mol)	95.6 (49.7–151)	45.3 (32.2–57.4)
Autoantibody positivity, % (*n*)		
GAD-positive	73.3 (11)	20 (1)
ICA-positive[a]	20 (3)	0 (0)
IAA-positive[b]	26.7 (4)	0 (0)
1 autoantibody	33.3 (5)	20 (1)
2 autoantibodies	33.3 (5)	0 (0)
3 autoantibodies	6.6 (1)	0 (0)

Unless indicated otherwise, values are mean (range)

[a] ICA, islet cell antibodies; [b] IAA, insulin autoantibodies

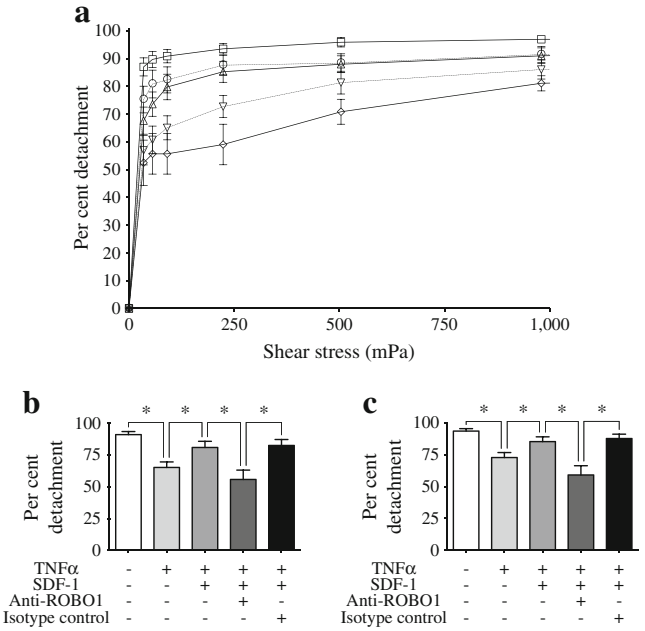

Fig. 4 (**a**) NOD/ShiLtJ T cells did not adhere to unstimulated MS1 endothelium (squares) in vitro. TNFα stimulation of MS1 cells (downward-pointing triangles) increased the resistance of T cells to shear-mediated detachment. Incubation of MS1 cells with SDF-1 reduced the adhesion of T cells to TNFα-activated endothelium (upward-pointing triangles). Incubation of T cells with a blocking antibody against ROBO1 blocked SDF-1-induced detachment from TNFα-activated endothelium (diamonds). (**b**) Per cent detachment at 91 mPa and (**c**) 224 mPa; *$p<0.05$

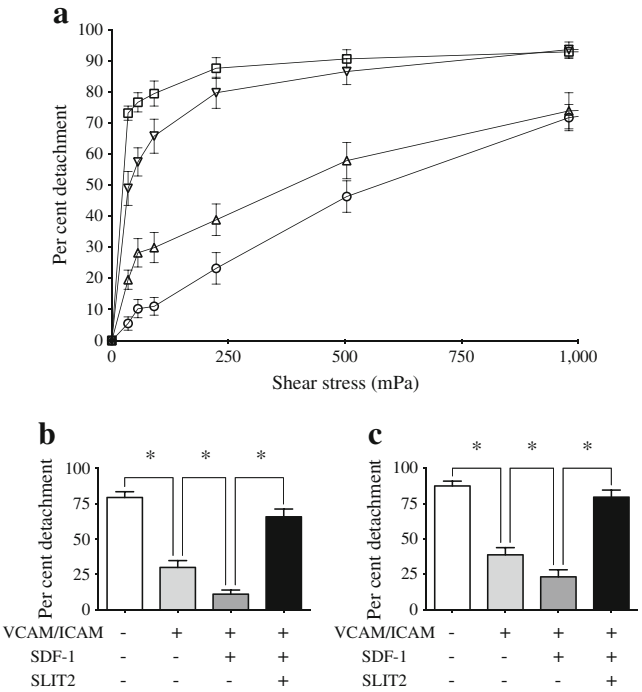

Fig. 5 (**a**) VCAM-1- and ICAM-1-coated plates (upward-pointing triangles) reduced the detachment of NOD/ShiLtJ T cells exposed to shear in vitro compared with BSA-coated controls (squares). T cells pretreated with SDF-1 exhibited reduced shear-mediated detachment from VCAM-1- and ICAM-1-coated plates (circles) compared with untreated T cells on the same plates (upward-pointing triangles), whereas the addition of SLIT2 to SDF-1-treated T cells promoted detachment from VCAM-1- and ICAM-1-coated plates (downward-pointing triangles). (**b**) Per cent detachment at 91 mPa and (**c**) 224 mPa; *$p<0.05$

Figure 4b, c more clearly illustrates the changes in detachment at 91 and 224 mPa, respectively.

SLIT2 reverses the effect of SDF-1 on T cell adhesion To confirm the importance of ROBO1–SLIT2 binding, we next examined the effect of SLIT2 on T cell adhesion. Because SLIT2 is expressed in endothelial cells, plates coated with recombinant ICAM-1 and VCAM-1 were used in a detachment assay with T cells treated with recombinant SLIT2 protein. As shown in Fig. 5a, ICAM-1- and VCAM-1-coated plates dramatically reduced T cell detachment compared with BSA controls. T cells pretreated with SDF-1 alone showed increased resistance to shear-mediated detachment compared with untreated T cells. However, cells treated with SDF-1 and SLIT2 showed a significant increase in detachment compared with cells treated with SDF-1 alone, demonstrating that SLIT2–ROBO1 binding regulates SDF-1-mediated chemorepulsion. Figure 5b, c illustrates the change in per cent detachment at 91 and 224 mPa, respectively.

SDF-1 peptide mimetic in vitro and in vivo Next, we examined whether a linear SDF-1 peptide mimetic containing the receptor-binding site could replicate the effect of full length SDF-1 in blocking adhesion of T cells to activated endothelium. MS1 cells were treated for 4 h with 10 ng/ml TNFα, followed by treatment for 10 min with an SDF-1 peptide mimetic at 200, 1,000 or 5,000 ng/ml. Cells were then used in a parallel plate flow chamber cell adhesion assay. Fluorescently labelled T cells obtained from NOD/ShiLtJ mice were flowed over the endothelial monolayers at 150 mPa. Figure 6a shows that TNFα induced adhesion five times greater than that of untreated endothelium and that this increase was significantly reduced by the SDF-1 peptide mimetic in a dose-dependent manner up to 5 μg/ml. Leucocyte adhesion videos were analysed to calculate the T cell rolling velocity and determine whether the decrease in firm adhesion was due to a decreased number of rolling cells. Consistent with our previous report [4], the SDF-1 peptide mimetic did not decrease the number of rolling cells (data not shown), nor did it affect the rolling velocity (Fig. 6b).

After proving the effectiveness of an SDF-1 peptide mimetic, we then used diabetogenic splenocytes in NOD/LtSz *Rag1*$^{-/-}$ mice to determine whether the CTCE-0214-stabilised, cyclic SDF-1 peptide designed for in vivo use altered the adoptive transfer of diabetes. Figure 6c–f shows the effectiveness of different doses of the SDF-1 mimetic peptide in delaying the onset of hyperglycaemia. At a dose of 10 mg/kg, the SDF-1 peptide mimetic effectively delayed adoptive transfer of diabetes, with a more beneficial effect being observed with once a week vs three times a week dosing. Together, these data confirm

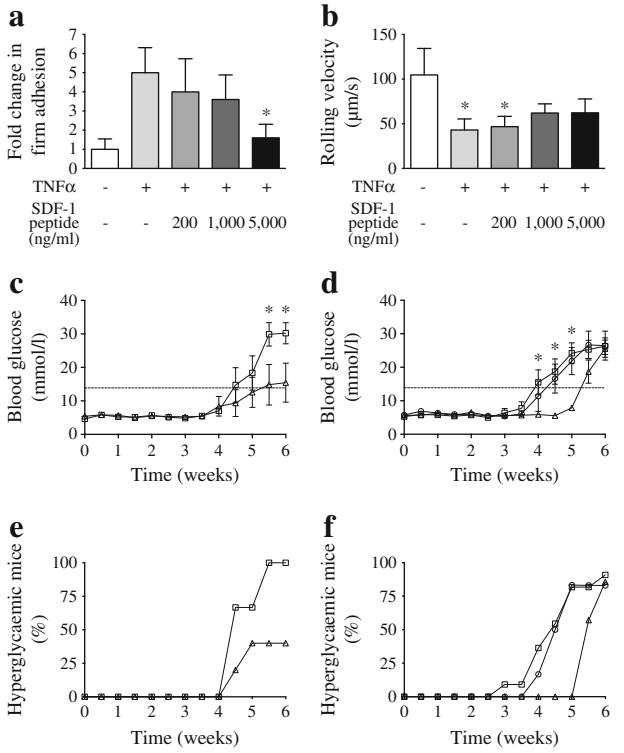

Fig. 6 (**a**) The SDF-1 peptide mimetic reversed TNFα-mediated adhesion in response to shear stress in vitro in a dose-dependent manner as measured by the fold change in the number of adherent cells captured by video; *$p<0.05$ vs TNFα alone. (**b**) The SDF-1 peptide mimetic did not significantly affect rolling velocity in TNFα-treated endothelial cells; *$p<0.05$ vs control. (**c**) CTCE-0214 slowed the development of diabetes in a NOD/LtSz *Rag1*$^{-/-}$ adoptive transfer model. At 5.5 and 6 weeks post-transfer, mice treated with 10 mg/kg CTCE-0214 once per week (upward-pointing triangles) showed significantly reduced glucose levels (*$p<0.05$) compared with PBS-treated mice (squares). The dashed line at 13.9 mmol/l glucose denotes the threshold for hyperglycaemia. (**d**) At 4 to 5 weeks post-transfer, mice treated with 10 mg/kg (upward-pointing triangles), but not those treated with 1 mg/kg (circles) CTCE-0214 three times per week, showed significantly reduced glucose levels (*$p<0.05$) compared with PBS treatment (squares). Dashed line, as above (**c**). Mice treated with CTCE-0214 at 10 mg/kg (upward-pointing triangles) both one (**e**) and three (**f**) times per week showed delayed development of hyperglycaemia compared with PBS treatment (squares)

the biological utility of SDF-1-mediated chemorepulsion responses in regulating the development of autoimmune diabetes.

Discussion

Having previously demonstrated a difference in the adhesion of T cells from C57BL/6J and NOD/ShiLtJ mice to SDF-1-treated endothelial cells in vitro [4], we investigated the levels of CXCR4 and ROBO1 in the T cells of these mice. CXCR4 levels in NOD/ShiLtJ T cells were significantly greater than those in C57BL/6J T cells. We found no significant cell surface CXCR7 expression on C57BL/6J or NOD/ShiLtJ T cells, suggesting that the difference in SDF-1-induced adhesion is likely to be mediated primarily by CXCR4. We found ROBO1 levels were significantly higher in NOD/ShiLtJ T cells, suggesting that increased SLIT2 and ROBO1 signalling could cause subsequent reversal of the adhesive effects of SDF-1.

Interestingly, we found that CXCR4 and ROBO1 protein expression increased over time in NOD/ShiLtJ CD3 T cells. This increase coincided with the development of hyperglycaemia, which, coupled with the fact that CXCR4 and SLIT2–ROBO1 dual engagement mediates chemorepulsion, might indicate a potential adaptive response to limit autoimmune leucocyte recruitment, as insulitis is known to occur many weeks before the onset of frank hyperglycaemia in NOD/ShiLtJ mice [23]. Surprisingly, steady-state mRNA levels of *Cxcr4* and *Robo1* did not increase with protein expression over time. In fact, *Cxcr4* mRNA significantly decreased over time for reasons not currently understood. Nonetheless, the divergence of changes in protein and mRNA expression strongly suggests that post-transcriptional regulation of gene expression could be responsible for the observed differences. Future studies will need to further investigate the reasons for these differences, as well as examining whether the upregulation of these proteins represents a potential protective response to regulate leucocyte recruitment.

We also measured expression of CXCR4 and ROBO1 in human T cells from diabetic and control participants to determine whether increased ROBO1 and CXCR4 expression was unique to the NOD/ShiLtJ mouse model. Interestingly, CXCR4 and ROBO1 expression was significantly elevated in type 1 diabetic patients versus non-diabetic controls. We also found that the difference between non-diabetic and type 1 diabetic participants was even more pronounced than that between C57BL/6J and NOD/ShiLtJ mice. Furthermore, while CXCR4 remained elevated in type 1 diabetic patients over 1 year after diagnosis, ROBO1 expression was reduced somewhat in long-term type 1 diabetic patients, suggesting that CXCR4 and ROBO1 expression profiles may serve as unique biomarkers for diagnosis or 'therapeutic windows' for type 1 diabetes, thus meriting future investigation.

After demonstrating that NOD/ShiLtJ mice have higher levels of T cell ROBO1 than their C57BL/6J counterparts, we investigated whether the blocking of SLIT2–ROBO1 binding with a blocking antibody against ROBO1 would restore the adhesive effect of SDF-1–CXCR4 binding. Our results clearly demonstrate that SLIT2–ROBO1 binding is involved in SDF-1-mediated detachment in NOD T cells, providing additional evidence that increased ROBO1 in NOD T cells might be responsible for this detachment. Next, by replacing endothelial cells with recombinant VCAM-1- and ICAM-1-coated plates, we were able to unequivocally demonstrate that SDF-1 increases NOD/ShiLtJ T cell adhesion in the absence of SLIT2–ROBO1 signalling and that the addition of SLIT2 mediates SDF-1-dependent

chemorepulsion of firm adhesion, as we had previously reported [4].

We also found that an SDF-1 peptide mimetic can reduce NOD/ShiLtJ T cell adhesion to islet endothelial cell monolayers in vitro. This is consistent with our previous findings, where adhesion of NOD/ShiLtJ T cells was reduced in the presence of full length SDF-1, whereas adhesion of C57BL/6J T cells was enhanced [4]. We then used the stabilised peptide agonist CTCE-0214 in an adoptive transfer model of type 1 diabetes, which is much more rapidly progressing than the spontaneous development of diabetes in NOD/ShiLtJ mice [24]; we found that CTCE-0214 significantly delayed the onset of hyperglycaemia. Together, these data clearly demonstrate that modulation of SDF-1 signalling responses for diabetogenic T cell recruitment can affect disease development in a model that is destined to develop diabetes, suggesting that a similar approach might be useful in altering T cell recruitment during spontaneous diabetes development.

Consistent with our results, Aboumrad et al showed that blockade of SDF-1–CXCR4 binding with AMD3100 accelerated the onset of diabetes in an adoptive transfer model and suggested that $CXCR4^+$ T cells were protective against diabetes [10]. This suggests that increased SDF-1 could potentially slow the development of disease, although others have shown that SDF-1 appears to accelerate disease development [12, 13]. Our data suggest that SDF-1 may be beneficial or detrimental during the development of diabetes, depending on the levels of T cell ROBO1 and locally expressed SLIT2, and require further investigation.

We used two doses of CTCE-0214 to examine therapeutic responses: 10 mg/kg, which proved to be beneficial, and 1 mg/kg, which had no effect. Moreover, the dosing frequency appeared to have some effect, as the once per week regimen showed a reduced incidence of hyperglycaemia up to 8 weeks (data not shown). It is possible that the decreased efficiency of the three times per week regimen of retro-orbital injections resulted from localised scarring or augmented immune-mediated clearance of the mimetic. Nonetheless, these data are encouraging and suggest that SDF-1 peptide mimetics may be able to alter the progression of autoimmune diabetes.

In summary, it is possible that higher levels of CXCR4, as seen in NOD/ShiLtJ mice and type 1 diabetic patients, cause increased SDF-1–CXCR4 signalling, resulting in a greater adhesion affinity of T cells for endothelial cells, which in turn would increase recruitment of T cells to the pancreas. Likewise, increased expression of ROBO1 may represent a complementary regulatory response to control the recruitment of overly aggressive T cells, resulting in a chemorepulsive effect for SDF-1. Many questions remain from these findings. For example, are CXCR4 and ROBO1 expression changes global across all T cells or associated with autoreactive T cells? Which T cell populations are involved (CD4 vs CD8)? Is divergent protein and mRNA expression for these molecules also seen in T cells from human type 1 diabetic patients, and if so, how might this occur? These questions aside, our results demonstrate that in vivo modulation through use of SLIT2 and ROBO1 peptides may prove useful in enhancing T cell chemorepulsive effects to delay the onset of diabetes. Future studies will need to examine this possibility further, as well as investigating molecular mechanisms of this novel regulatory pathway of diabetic T cell recruitment.

Acknowledgements The CTCE-0214 peptide mimetic was a kind gift from British Canadian BioSciences. The ROBO1 antibody (vRobo1), developed by Janne Balsamo, Jack Lilien and Jinseol Rhee (Department of Biological Sciences, University of Iowa, Iowa City, IA, USA), was obtained from the Developmental Studies Hybridoma Bank, developed under the auspices of the National Institute of Child Health and Human Development and maintained by The University of Iowa, Department of Biology, Iowa City, IA, USA.

Funding This work was supported by a grant from the American Diabetes Association (1-10-BS-84 to CGK). JDG, RM and CGK have filed a provisional patent on the use of CXCR4 and ROBO1 as biomarkers of type 1 diabetes and the use of peptide mimetics to inhibit diabetogenic T cell recruitment.

Duality of interest The authors declare that there is no duality of interest associated with this manuscript.

Contribution statement JDG, EMM and WCD acquired and analysed data, wrote the manuscript and approved the final version to be published. SCB, RM and NG contributed substantially to the acquisition of data, reviewed the manuscript and approved the final version to be published. CGK designed the research, wrote and edited the manuscript, managed the research project, obtained grant funding and approved the final version to be published.

References

1. Balabanian K, Lagane B, Infantino S et al (2005) The chemokine SDF-1/CXCL12 binds to and signals through the orphan receptor RDC1 in T lymphocytes. J Biol Chem 280:35760–35766
2. Saini V, Marchese A, Majetschak M (2010) CXC chemokine receptor 4 is a cell surface receptor for extracellular ubiquitin. J Biol Chem 285:15566–15576
3. Hartmann TN, Grabovsky V, Pasvolsky R et al (2008) A crosstalk between intracellular CXCR7 and CXCR4 involved in rapid CXCL12-triggered integrin activation but not in chemokine-triggered motility of human T lymphocytes and CD34+ cells. J Leukoc Biol 84:1130–1140
4. Sharp CD, Huang M, Glawe J et al (2008) Stromal cell-derived factor-1/CXCL12 stimulates chemorepulsion of NOD/LtJ T cell adhesion to islet microvascular endothelium. Diabetes 57:102–112
5. Papeta N, Chen T, Vianello F et al (2007) Long-term survival of transplanted allogeneic cells engineered to express a T cell chemorepellent. Transplantation 83:174–183
6. Vianello F, Papeta N, Chen T et al (2006) Murine B16 melanomas expressing high levels of the chemokine stromal-derived factor-1/CXCL12 induce tumor-specific T cell chemorepulsion and escape from immune control. J Immunol 176:2902–2914
7. Zhong R, Law P, Wong D, Merzouk A, Salari H, Ball ED (2004) Small peptide analogs to stromal derived factor-1 enhance chemotactic migration of human and mouse hematopoietic cells. Exp Hematol 32:470–475

8. Fan H, Wong D, Ashton SH, Borg KT, Halushka PV, Cook JA (2012) Beneficial effect of a CXCR4 agonist in murine models of systemic inflammation. Inflammation 35:130–137
9. Faber A, Roderburg C, Wein F et al (2007) The many facets of SDF-1alpha, CXCR4 agonists and antagonists on hematopoietic progenitor cells. J Biomed Biotechnol 2007:26065
10. Aboumrad E, Madec AM, Thivolet C (2007) The CXCR4/CXCL12 (SDF-1) signalling pathway protects non-obese diabetic mouse from autoimmune diabetes. Clin Exp Immunol 148:432–439
11. Yano T, Liu Z, Donovan J, Thomas MK, Habener JF (2007) Stromal cell derived factor-1 (SDF-1)/CXCL12 attenuates diabetes in mice and promotes pancreatic beta-cell survival by activation of the prosurvival kinase Akt. Diabetes 56:2946–2957
12. Zhao Y, Guo C, Hwang D et al (2010) Selective destruction of mouse islet beta cells by human T lymphocytes in a newly-established humanized type 1 diabetic model. Biochem Biophys Res Commun 399:629–636
13. Matin K, Salam MA, Akhter J, Hanada N, Senpuku H (2002) Role of stromal-cell derived factor-1 in the development of autoimmune diseases in non-obese diabetic mice. Immunology 107:222–232
14. Wu JY, Feng L, Park HT et al (2001) The neuronal repellent Slit inhibits leukocyte chemotaxis induced by chemotactic factors. Nature 410:948–952
15. Guan H, Zu G, Xie Y et al (2003) Neuronal repellent Slit2 inhibits dendritic cell migration and the development of immune responses. J Immunol 171:6519–6526
16. Hussain SA, Piper M, Fukuhara N et al (2006) A molecular mechanism for the heparan sulfate dependence of slit-robo signaling. J Biol Chem 281:39693–39698
17. Chalasani SH, Sabol A, Xu H et al (2007) Stromal cell-derived factor-1 antagonizes slit/robo signaling in vivo. J Neurosci 27:973–980
18. Chen B, Blair DG, Plisov S et al (2004) Cutting edge: bone morphogenetic protein antagonists Drm/Gremlin and Dan interact with Slits and act as negative regulators of monocyte chemotaxis. J Immunol 173:5914–5917
19. Prasad A, Qamri Z, Wu J, Ganju RK (2007) Slit-2/Robo-1 modulates the CXCL12/CXCR4-induced chemotaxis of T cells. J Leukoc Biol 82:465–476
20. Fang K, Bruce M, Pattillo CB et al (2011) Temporal genomewide expression profiling of DSS colitis reveals novel inflammatory and angiogenesis genes similar to ulcerative colitis. Physiol Genomics 43:43–56
21. Tudan C, Willick GE, Chahal S et al (2002) C-terminal cyclization of an SDF-1 small peptide analogue dramatically increases receptor affinity and activation of the CXCR4 receptor. J Med Chem 45:2024–2031
22. Glawe JD, Patrick DR, Huang M, Sharp CD, Barlow SC, Kevil CG (2009) Genetic deficiency of Itgb2 or ItgaL prevents autoimmune diabetes through distinctly different mechanisms in NOD/LtJ mice. Diabetes 58:1292–1301
23. Giarratana N, Penna G, Adorini L (2007) Animal models of spontaneous autoimmune disease: type 1 diabetes in the nonobese diabetic mouse. Methods Mol Biol 380:285–311
24. Shultz LD, Lang PA, Christianson SW et al (2000) NOD/LtSz-Rag1null mice: an immunodeficient and radioresistant model for engraftment of human hematolymphoid cells, HIV infection, and adoptive transfer of NOD mouse diabetogenic T cells. J Immunol 164:2496–2507